Gastrointestinal Tumors

ARTICLE

Open Access

https://doi.org/10.48130/git-0026-0001

Gastrointestinal Tumors **2026**, 13: e004

Tumor-associated macrophage density as a predictive biomarker for survival benefit from adjuvant chemotherapy in gastric cancer

Wen Zhu[#], Qing Tao[#], Kebin Dong, Qingyuan Song, Tao Feng, Xiaoqin Li and Deqiang Wang*

Cancer Center, Affiliated Hospital of Jiangsu University, Zhenjiang 212000, China

[#] Authors contributed equally: Wen Zhu, Qing Tao

* Correspondence: deqiang_wang@aliyun.com (Wang D)

Abstract

Adjuvant chemotherapy (ACT) is the standard treatment for Stage II–III gastric cancer after surgery, but biomarkers to guide patient selection are lacking. This study investigated whether spatial quantification of specific immune cell subsets could serve as such a biomarker. We performed multiplex immunofluorescence on postoperative specimens from 47 patients with Stage II–III gastric cancer. Immune cells were quantified in the tumor parenchyma and stroma. Their associations with overall survival (OS) and disease-free survival (DFS) were analyzed. High M1 macrophage density (in both the parenchyma and stroma), high parenchymal $CD56^{dim}$ natural killer (NK)-cell density, and high stromal M2 macrophage density were significantly associated with better OS and DFS in patients receiving ACT. Importantly, only patients with high M2 macrophage density derived a significant OS benefit from ACT compared with observation alone, in either the parenchyma or stroma (e.g., parenchyma: hazard ratio [HR] = 0.28, 95% confidence interval [CI]: 0.08–0.96, p = 0.029; stroma: HR = 0.14, 95% CI: 0.03–0.66, p = 0.003). A significant DFS benefit from ACT was also observed in patients with high stromal M2 density (HR = 0.22, 95% CI: 0.06–0.86, p = 0.016). No other immune cell subset consistently predicted the benefit of ACT. In conclusion, the pre-existing density and spatial distribution of tumor-associated macrophages are key determinants of prognosis and ACT's efficacy in gastric cancer.

Citation: Zhu W, Tao Q, Dong K, Song Q, Feng T, et al. 2026. Tumor-associated macrophage density as a predictive biomarker for survival benefit from adjuvant chemotherapy in gastric cancer. *Gastrointestinal Tumors* 13: e004 https://doi.org/10.48130/git-0026-0001

Introduction

Gastric cancer is the fourth most commonly diagnosed malignancy worldwide and represents the fourth leading cause of cancer-related death[1]. Although surgery remains the primary curative treatment, postoperative recurrence rates remain high[2]. Postoperative adjuvant chemotherapy (ACT), including regimens such as XELOX (oxaliplatin + capecitabine) and SOX (oxaliplatin + S-1), has significantly improved both disease-free survival (DFS) and overall survival (OS) in gastric cancer patients[3]. Nevertheless, recurrence still occurs in nearly half of all patients.

With the advent of immunotherapy for gastric cancer, the recent ATTRACTION-5 trial investigating adjuvant immunotherapy failed to demonstrate a survival benefit[4]. Thus, ACT remains the standard postoperative treatment for Stage II–III gastric cancer[5]. The identification of biomarkers capable of selecting patients who are likely (or unlikely) to benefit from ACT could substantially improve the efficacy of adjuvant therapy.

Recent advances in high-throughput sequencing and the expansion of multiomics studies have enabled detailed molecular characterization of cancers, profoundly enriching our understanding of tumor biology[6–8]. A major focus of these efforts is the tumor microenvironment (TME). Using cell-surface markers and transcriptomic data, researchers have developed computational algorithms to deconvolve the cellular composition of the TME[9–14]. There is growing evidence that TME-derived scores and the related metrics can serve as novel biomarkers for predicting prognosis and the response to treatment[15–17]. However, bioinformatics-based estimations often deviate from the actual TME, and most current algorithms still lack large-scale, multicancer experimental validation.

In this study, we employed multiplex immunofluorescence (mIF) to quantify immune cell densities in postoperative gastric cancer specimens and assessed their influence on prognosis and survival benefit from ACT. A high density of M1 macrophages, both in the tumor epithelium and stroma, was strongly associated with improved prognosis. Similarly, the density of the $CD56^{dim}$ natural killer (NK)-cell subset in the parenchyma and M2 macrophages in the stroma also predicted clinical outcomes. Notably, only patients with high M2 macrophage infiltration derived a significant OS benefit from ACT regardless of the compartment, whereas those with low M2 infiltration did not. These results suggest that immune cell infiltration levels may serve as both prognostic and predictive biomarkers for ACT in postoperative gastric cancer.

Methods

Patients

This study utilized a previously described multiomics gastric cancer cohort from the Affiliated Hospital of Jiangsu University (AHJU)[18–20]. From this cohort, we selected samples for mIF staining on the basis of the following inclusion criteria: Histopathologically confirmed gastric adenocarcinoma, D2 radical surgery with R0 resection,Stage II–III disease (indicating eligibility for ACT ≥ T2 and/or node-positive, M0), complete postoperative treatment records, and adequate tissue quality and quantity for mIF analysis. Exclusion criteria included prior neoadjuvant therapy, death within 3 months after surgery, and concurrent primary malignancies. Clinical and pathologic staging adhered to the American Joint Committee on Cancer criteria. Written informed consent was obtained from all participants. The study complied with the principles of the Declaration of Helsinki and was approved by the Ethics Committee of AHJU.

Multiplex immunofluorescence staining

To characterize the spatial architecture of tumor-infiltrating immune cells, we performed seven-color mIF combined with multispectral microscopy. Formalin-fixed, paraffin-embedded tissue sections were deparaffinized, subjected to heat-induced epitope retrieval, and stained using the PANO 7-plex immunohistochemistry (IHC) kit (Panovue, Beijing, China) according to the manufacturer's protocol. The antibody panel included pan-cytokeratin (CST4545, Cell Signaling Technology) to label carcinoma cells, CD8 (CST70306) for cytotoxic T lymphocytes, CD56 (CST3576) for NK cells, and CD68 (BX50031, Biolynx) and HLA-DR (ab92511, Abcam) for macrophages. NK cells were categorized into two functional subsets according to the CD56 signal's intensity: $CD56^{dim}$ (cytotoxic, low membrane fluorescence) and $CD56^{bright}$ (immunoregulatory, high-intensity staining). Macrophages were classified as pro-inflammatory M1 (CD68 + HLA-DR+) or immunosuppressive M2 (CD68 + HLA-DR−). S100 (ab52642) staining was used to demarcate the invasive margin from the tumor parenchyma, as previously described[21].

Following sequential tyramide signal amplification and 4′,6-diamidino-2-phenylindole (DAPI) counterstaining, whole-slide images were acquired using the Mantra quantitative pathology workstation (PerkinElmer, Waltham, MA, USA). A spectral library generated from single-fluorophore references was applied to unmix raw image stacks and remove autofluorescence. The resulting seven-channel images were analyzed with inForm software (PerkinElmer) for automated cell segmentation, phenotypic classification, and spatial mapping, yielding single-cell level counts for each immune subset.

Endpoints

OS was defined as the time from surgery to death from any cause. DFS was defined as the time from surgery to the first documented recurrence, new malignancy, or death from any cause, whichever occurred first.

Statistical analysis

Clinicopathologic characteristics were compared between groups using the χ^2 test. Survival analyses were conducted using Kaplan–Meier curves and log-rank tests. Hazard ratios (HRs) with 95% confidence intervals (CIs) were calculated. All statistical analyses and graphics were generated using R software (version 4.5.0) and the relevant packages. A two-sided p-value of <0.05 was considered to be statistically significant.

Results

Patient characteristics

The study included 47 patients and their tissue specimens. Among them, 25 received postoperative ACT, all with the XELOX regimen. The cohort was predominantly male (n = 37, 78.7%), with only 10 female patients. Our population included 29 patients (61.7%) who were elderly (≥65 years), and 18 were under 65 years old. Poorly differentiated (Grade III) tumors were present in 37 cases, whereas 10 were well to moderately differentiated (Grades I/II). In total, 34 patients had Stage III disease, and 13 had Stage II disease. Clinicopathologic characteristics did not differ significantly between patients who received ACT and those who did not (Table 1). Typical mIF staining micrographs can be seen in Fig. 1. Immune cell subset densities showed no significant association with any clinicopathologic variable in either the tumor parenchyma (Supplementary Fig. S1) or stroma (Supplementary Fig. S2).

Table 1. Patient characteristics.

Variable	Group	Adjuvant chemotherapy		p-Value
		No	Yes	
Age (years)	< 65	8 (36.4)	10 (40.0)	0.798
	≥ 65	14 (63.6)	15 (60.0)	
Sex	Female	3 (13.6)	7 (28.0)	0.230
	Male	19 (86.4)	18 (72.0)	
Histological grade	I/II	5 (22.7)	5 (20.0)	0.820
	III	17 (77.3)	20 (80.0)	
Stage	II	7 (31.8)	6 (24.0)	0.550
	III	15 (68.2)	19 (76.0)	

Immune infiltration and OS in patients receiving ACT

Immune cell densities in the tumor parenchyma and stroma were dichotomized into high and low groups according to their median values. Among ACT-treated patients, high M1 macrophage density in the parenchyma was associated with a significantly longer OS (Fig. 2a): Median OS was not reached in the high-density group, compared with 18 months (95% CI: 11.1–24.9) in the low-density group (p = 0.006; HR = 0.16, 95% CI: 0.04–0.70). A similar effect was observed for $CD56^{dim}$ NK-cell density in the parenchyma (Fig. 2d): Median OS was not reached in the high-density group, versus 32 months (11.2–52.8) in the low-density group (p = 0.006; HR = 0.15, 95% CI: 0.03–0.76). By contrast, densities of M2 macrophages, $CD56^{bright}$ NK-cells, and $CD8^+$ T-cells in the parenchyma showed no significant prognostic impact (Fig. 2b, c, e).

In the stroma, high M1 macrophage density remained a significant prognostic factor (p = 0.006; Fig. 3a), whereas $CD56^{dim}$ density did not (p = 0.550; Fig. 3d). High stromal M2 macrophage density was associated with improved OS (Fig. 3b): Median OS was not reached in the high-density group, compared with 38 months (12.2–63.8) in the low-density group (p = 0.006; HR = 0.23, 95% CI: 0.05–1.13). Notably, M1 density classifications were nearly identical between the parenchyma and stroma, differing in only two patients. $CD56^{bright}$ and $CD8^+$ T-cell densities in the stroma again showed no significant association with OS (Fig. 3c, e).

Immune infiltration and DFS in patients with ACT

We next assessed the relationship between immune infiltration and DFS. In the parenchyma, high M1 macrophage density was associated with significantly longer DFS (Supplementary Fig. S3a): Median DFS was not reached in the high-density group, versus 11 months (0–23.5) in the low-density group (p = 0.014; HR = 0.22, 95% CI: 0.06–0.84). Similarly, high $CD56^{dim}$ NK-cell density predicted improved DFS (Supplementary Fig. S3d): Median DFS was not reached in the high-density group, compared with 20 months (15.3–24.7) in the low-density group (p = 0.007; HR = 0.16, 95% CI: 0.03–0.76). No significant DFS associations were observed for M2 macrophages, $CD56^{bright}$ NK-cells, or $CD8^+$ T-cells in the parenchyma (Supplementary Fig. S3b, S3c, S3e).

In the stroma, M1 macrophage density again significantly influenced DFS (p = 0.014; Supplementary Fig. S4a). M2 macrophage density showed a nonsignificant trend toward DFS benefit (p = 0.094; Supplementary Fig. S4b), whereas $CD56^{bright}$, $CD56^{dim}$, and $CD8^+$ T-cell densities had no effect on DFS (Supplementary Fig. S4c–S4e).

Immune infiltration and OS benefit from ACT

We evaluated the benefit of ACT according to immune infiltration levels. In the parenchyma, patients with high M2 macrophage

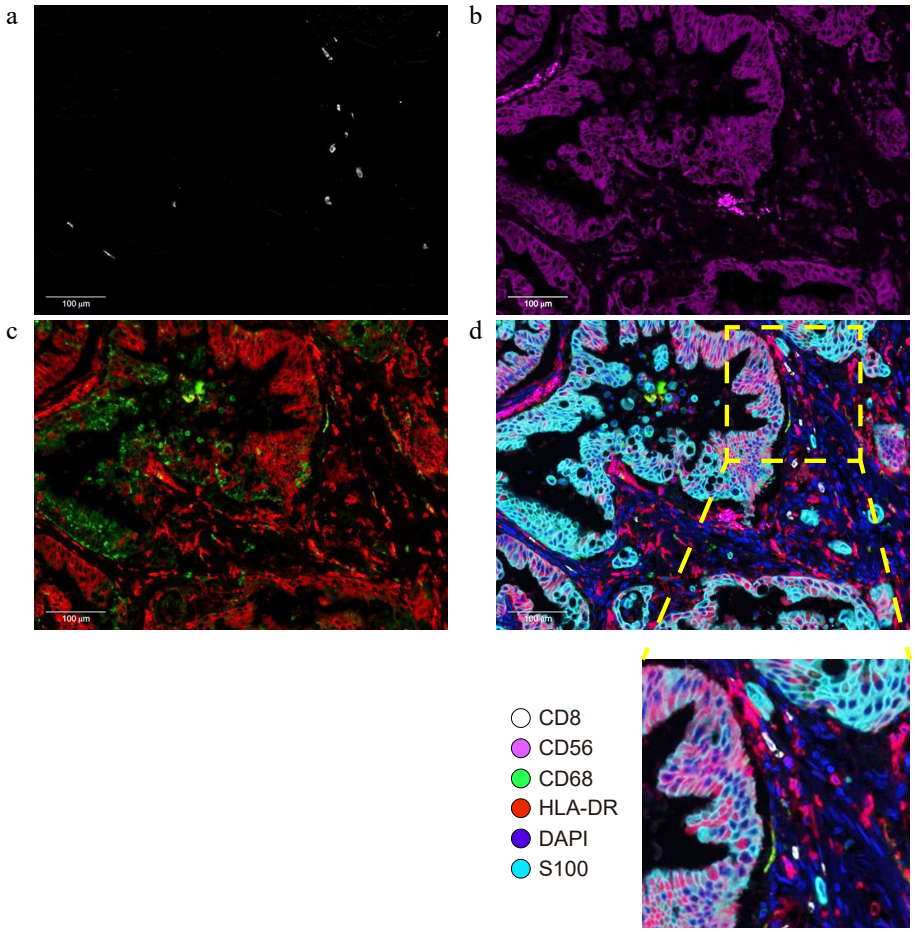

Fig. 1 Typical photomicrographs of multiple immunofluorescence staining: (a) $CD8^+$ (white); (b) $CD56^+$ (purple); (c) $CD68^+$ (green) and HLA-DR (red); and (d) Reconstructed image after removal of autofluorescence and local enlargement. The lower right panel of (d) is a 4× magnified image of the selected region.

density derived a significant OS benefit from ACT ($p = 0.029$; Fig. 4b): Median OS was not reached in the ACT group versus 17 months (0–34.0) in the observation group (HR = 0.28, 95% CI: 0.08–0.96). Among patients with high M1 density, a trend toward OS benefit from ACT was observed, but it was not statistically significant ($p = 0.15$; Fig. 4a). ACT did not significantly affect OS in any high-density $CD56^{bright}$, $CD56^{dim}$, or $CD8^+$ T-cell subgroups (Fig. 4c–e). In all low-density immune cell subsets, ACT did not significantly prolong OS (Supplementary Fig. S5a–S5e), although a nonsignificant trend was noted for patients with a low $CD56^{bright}$ density ($p = 0.12$; Supplementary Fig. S5c).

In the stroma, high M2 macrophage density again predicted ACT benefit (Fig. 5b): Median OS was not reached with ACT versus 17 months (6.2–27.8) without it (HR = 0.14, 95% CI: 0.03–0.66). No significant OS benefit was observed in other high-density stromal immune subsets (Fig. 5a, c–e). Similarly, ACT conferred no OS benefit in any low-density stromal subgroup (Supplementary Fig. S6a–S6e), though a nonsignificant trend was again observed for low $CD56^{bright}$ density ($p = 0.16$; Supplementary Fig. S6c).

Immune infiltration and DFS benefit from ACT

The impact of immune infiltration on DFS benefit from ACT mirrored that for OS. In the parenchyma, patients with high M2 infiltration showed a marked DFS benefit from ACT, though the difference did not reach statistical significance ($p = 0.07$; Supplementary Fig. S7b). No significant DFS benefit was observed in other high-density immune subsets (Supplementary Fig. S7a, S7c–S7e), although a trend was noted for high M1 infiltration ($p = 0.22$; Supplementary Fig. S7a). Among low-density subsets, only the $CD56^{bright}$ group showed a borderline trend toward prolonged DFS with ACT ($p = 0.18$; Supplementary Fig. S8c); all other low-density groups showed no benefit (Supplementary Fig. S8a, S8b, S8d, S8e).

In the stroma, ACT significantly prolonged DFS in patients with high M2 infiltration (Supplementary Fig. S9b): Median DFS was not reached with ACT, compared with 10 months (2.3–17.7) without it (HR = 0.22, 95% CI: 0.06–0.86). No other high-density stromal subset showed a significant DFS benefit (Supplementary Fig. S9a, S9c–S9e). Similarly, all low-density stromal subsets did not benefit from ACT (Supplementary Fig. S10a–S10e), except for a nonsignificant trend in the $CD56^{bright}$ low-density group ($p = 0.2$; Supplementary Fig. S10c).

Discussion

This study underscores the dual role of immune infiltration in gastric cancer, impacting both patients' prognosis and the response to postoperative ACT. Specifically, M1 macrophage density serves as a prognostic indicator, whereas M2 macrophage density predicts a survival benefit from ACT, irrespective of their localization in the tumor's parenchyma or stroma. These findings provide potential biomarkers for personalizing ACT in gastric cancer, which may improve therapeutic efficacy and reduce overtreatment.

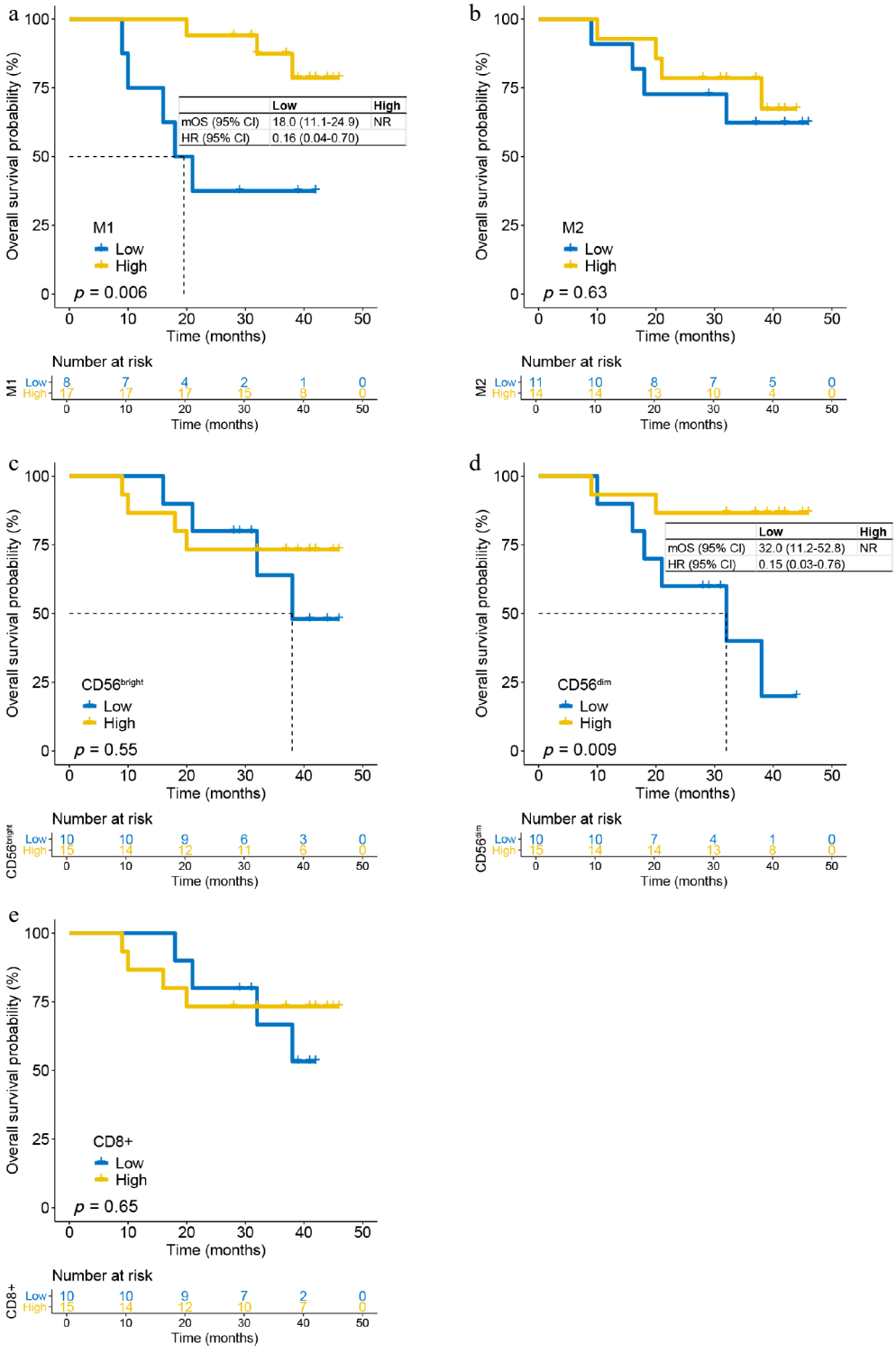

Fig. 2 The density of immune infiltrating cells in the tumor parenchyma and OS in patients receiving adjuvant chemotherapy. (a) M1 cells; (b) M2 cells; (c) CD56^{bright} cells; (d) CD56^{dim} cells; (e) CD8^{+} T-cells.

Computational estimation of immune infiltration from bulk RNA-Seq data using algorithms such as CIBERSORT, xCell, MCP-counter, TIMER, quanTIseq, and IPS has become a standard method for characterizing the TME[9–14]. Subtyping tumors by immune infiltration patterns, identifying differentially expressed genes, and deriving gene signatures via machine learning can yield risk scores that predict prognosis and treatment efficacy in gastric cancer[15–17]. Nevertheless, bioinformatics-based TME assessments have inherent limitations. The current algorithms rely almost exclusively on high-throughput mRNA data, which demand high-quality specimens and incur substantial costs. Moreover, these tools have not been rigorously validated against large multicancer cohorts measured by orthogonal methods; for example, the concordance between *in silico* immune estimates and mIF quantification in gastric cancer remains uncertain. Moreover, bulk sequencing fails to differentiate between parenchymal and stromal compartments, whereas

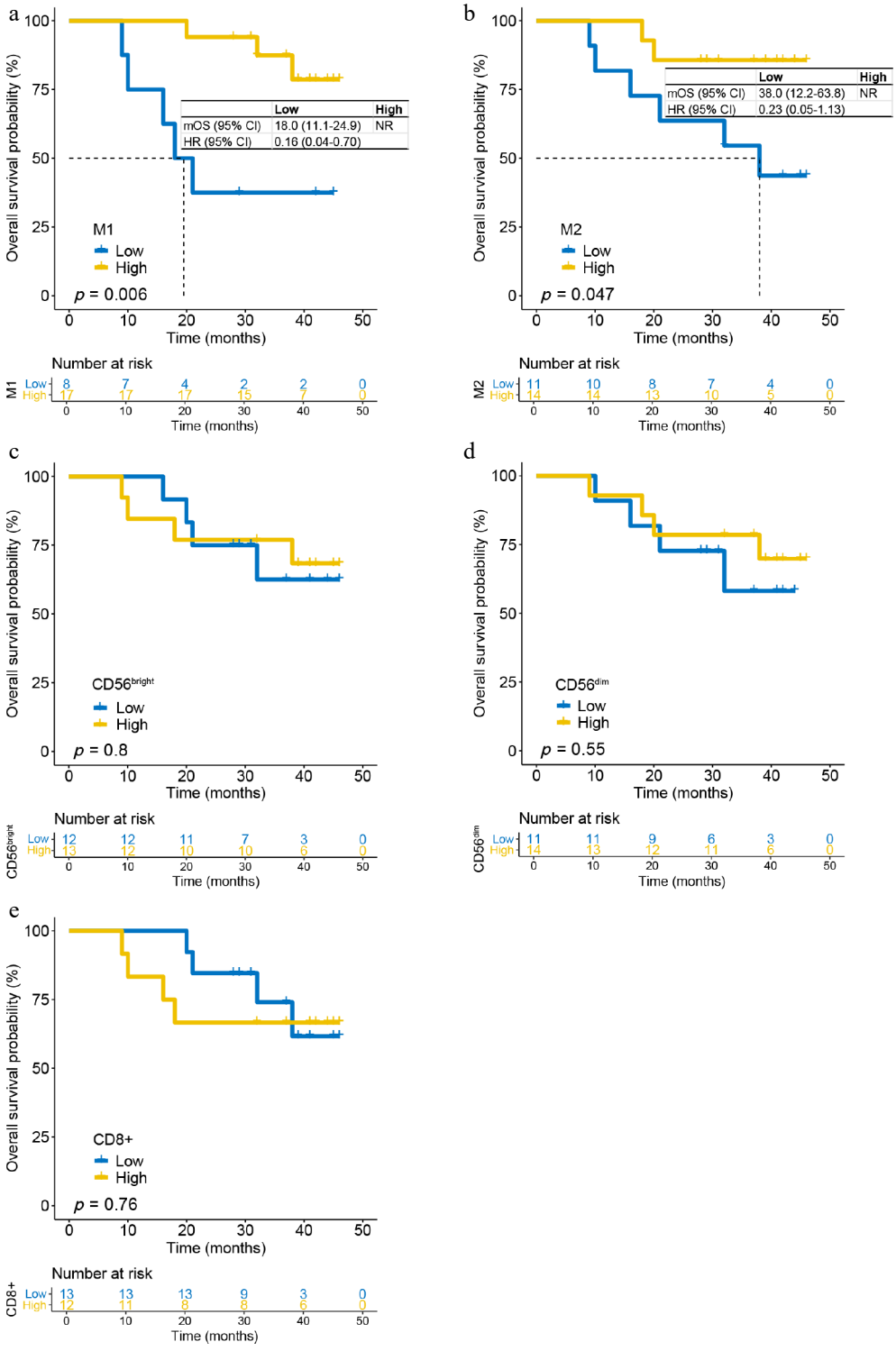

Fig. 3 The density of immune infiltrating cells in the tumor stroma and OS in patients receiving adjuvant chemotherapy. (a) M1 cells; (b) M2 cells; (c) $CD56^{bright}$ cells; (d) $CD56^{dim}$ cells; and (e) $CD8^{+}$ T-cells.

single-cell or spatial transcriptomics are currently not feasible for routine clinical application. In contrast, our mIF-based approach bridges this translational gap by providing a clinically actionable alternative for assessing immune infiltration.

Our results underscore the clinical relevance of the macrophages in gastric cancer. As key components of the mononuclear phagocyte system, macrophages regulate immunity, clear pathogens, promote wound healing, and modulate angiogenesis[22]. Stimulated by distinct cytokine milieus, they polarize into two functionally opposing states, namely proinflammatory, tumor-suppressive M1 macrophages and anti-inflammatory, tumor-supportive M2 macrophages[23]. Within the TME, these cells are collectively known as tumor-associated macrophages (TAMs). We found that a high M1-TAM density correlates with favorable prognosis, reflecting their antitumor activity. Conversely, a high M2-TAM density identifies patients who would benefit from ACT, likely because chemotherapy

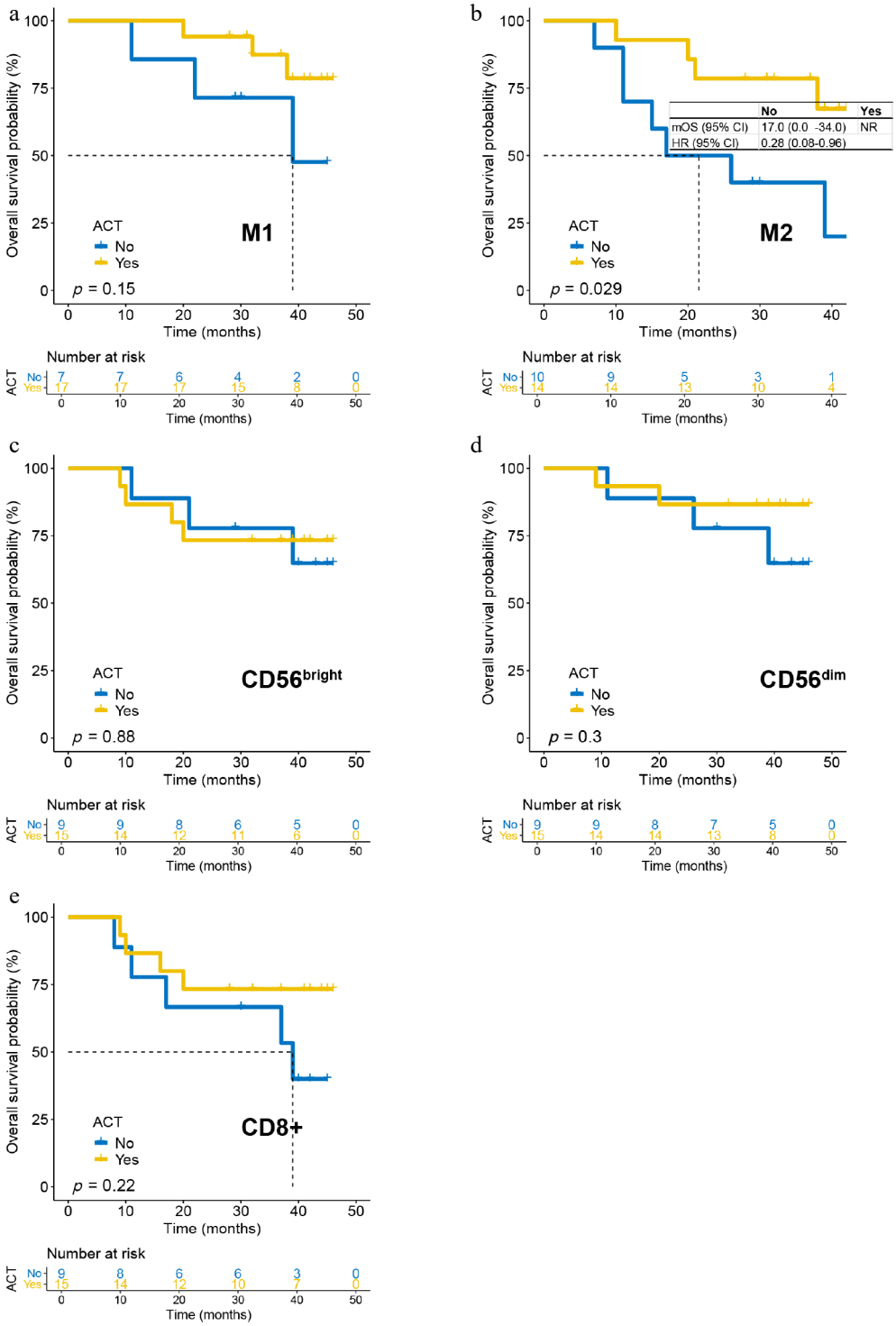

Fig. 4 The impact of ACT on OS in patients with high-density immune infiltrating cells in the tumor parenchyma. (a) M1 cells; (b) M2 cells; (c) $CD56^{bright}$ cells; (d) $CD56^{dim}$ cells; and (e) $CD8^+$ T-cells.

depletes M2 cells and reprograms the immune milieu. Importantly, both M1 and M2 densities were informative, regardless of the spatial context, suggesting that TAMs influence tumor progression through both direct cellular interactions and microenvironmental modulation. TAMs engage in crosstalk with cancer cells, adipocytes, and stromal elements to alter metabolism, inflammation, and immune activity, thereby shaping the tumor's evolution[24]. They also secrete enzymes involved in nicotinamide metabolism, which fine-tune $CD8^+$ T-cells' function and influence the response to immunotherapy in gastric cancer[25].

We also evaluated NK-cell subsets and found that the density of $CD56^{dim}$ in the parenchyma carries prognostic significance. NK-cells are among the body's principal antitumor effectors, comprising roughly 15% of the circulating lymphocytes. Their tumoricidal arsenal includes the release of perforin-containing cytotoxic granules, the secretion of pro-apoptotic cytokines, and the mediation of

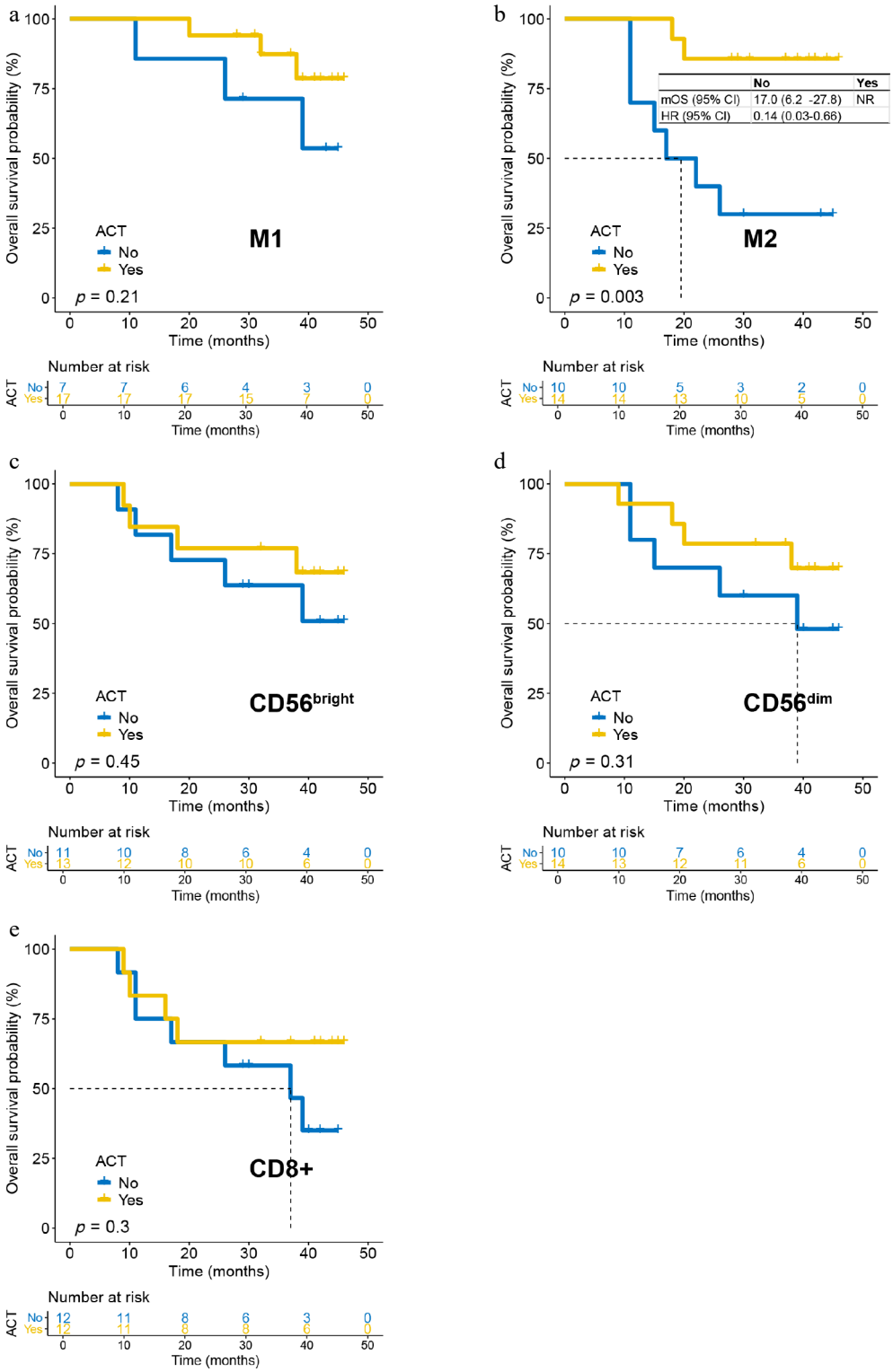

Fig. 5 The impact of adjuvant chemotherapy on overall survival in patients with high-density immune infiltrating cells in the tumor stroma. (a) M1 cells; (b) M2 cells; (c) CD56^{bright} cells; (d) CD56^{dim} cells; and (e) CD8^{+} T cells.

antibody-dependent cellular cytotoxicity[26]. Human NK-cells are subdivided into CD56^{dim} and CD56^{bright} subsets. CD56^{dim} cells account for ~90 % of peripheral NK-cells and are considered to be mature, equipped for both cytokine production and potent cytotoxicity, whereas CD56^{bright} cells (~10 %) are less mature and primarily secrete cytokines[27]. Intriguingly, the prognostic value of CD56^{dim} cells was restricted to the tumor parenchyma; their abundance in the stroma had no impact on the outcomes. This compartment-specific effect suggests that CD56^{dim} NK-cells must physically infiltrate the malignant nest to exert their protective function.

Our study has several limitations. First, the small sample size meant that some subgroup analyses showed only trends without

reaching statistical significance; expansion to a larger cohort is therefore necessary. Second, the ACT and observation groups were not matched for clinicopathologic characteristics, introducing potential bias. Third, this is a retrospective analysis whose findings must be confirmed by prospective randomized controlled trials. Finally, the oncologic outcomes were determined by multiple intertwined factors; we did not perform multivariable modeling, mainly because the limited number of events would have rendered such analysis underpowered.

Conclusions

In summary, this study demonstrates that pretreatment immune cell infiltration in gastric cancer influences both prognosis and the benefit of ACT, offering a potential tool for personalizing treatment. Future directions include: (1) validating these findings in larger, multicenter cohorts, (2) conducting prospective trials using immune infiltration to guide ACT-related decisions, and (3) elucidating the biological mechanisms by which macrophage density modulates the treatment response.

Ethical statements

The study was conducted in accordance with the Declaration of Helsinki, and all procedures were approved by the Institutional Review Board of Affiliated Hospital of Jiangsu University.

Author contributions

The authors confirm contribution to the paper as follows: Study conception and design: Zhu W, Tao Q, and Wang D; data collection: Zhu W, Tao Q, Dong K, Song Q, Feng T, and Wang D; analysis and interpretation of results: Zhu W, Tao Q, Dong K, Li X, and Wang D; draft manuscript preparation: Zhu W and Wang D. All authors reviewed the results and approved the final version of the manuscript.

Data availability

All data generated or analyzed during this study are included in this published article and its supplementary information files. Further data relevant to the study may be obtained from the corresponding author upon reasonable request.

Acknowledgments

The study was funded by The Natural Science Foundation of Jiangsu Province (BK20231252) and the Key Medical Research Projects of Jiangsu Provincial Health Commission (K2023026).

Conflict of interest

The authors declare that they have no conflict of interest.

Supplementary information accompanies this paper online at: https://doi.org/10.48130/git-0026-0001.

Dates

Received 1 October 2025; Revised 15 December 2025; Accepted 13 January 2026; Published online 27 February 2026

References

[1] Bray F, Laversanne M, Sung H, Ferlay J, Siegel RL, et al. 2024. Global cancer statistics 2022: GLOBOCAN estimates of incidence and mortality worldwide for 36 cancers in 185 countries. *CA: A Cancer Journal for Clinicians* 74:229–263

[2] Sundar R, Nakayama I, Markar SR, Shitara K, van Laarhoven H, et al. 2025. Gastric cancer. *The Lancet* 405:2087–2102

[3] Takayama T, Tsuji Y. 2023. Updated Adjuvant Chemotherapy for Gastric Cancer. *Journal of Clinical Medicine* 12:6727

[4] Kang YK, Terashima M, Kim YW, Boku N, Chung HC, et al. 2024. Adjuvant nivolumab plus chemotherapy versus placebo plus chemotherapy for stage III gastric or gastro-oesophageal junction cancer after gastrectomy with D2 or more extensive lymph-node dissection (ATTRACTION-5): a randomised, multicentre, double-blind, placebo-controlled, phase 3 trial. *The Lancet Gastroenterology & Hepatology* 9:705–717

[5] Wang FH, Zhang XT, Tang L, Wu Q, Cai MY, et al. 2024. The Chinese Society of Clinical Oncology (CSCO): Clinical guidelines for the diagnosis and treatment of gastric cancer, 2023. *Cancer Communications* 44:127–172

[6] Hirata Y, Noorani A, Song S, Wang L, Ajani JA. 2023. Early stage gastric adenocarcinoma: clinical and molecular landscapes. *Nature Reviews Clinical Oncology* 20:453–469

[7] Ma H, Srivastava S, Ho SWT, Xu C, Lian BSX, et al. 2025. Spatially resolved tumor ecosystems and cell states in gastric adenocarcinoma progression and evolution. *Cancer Discov* 15:767–792

[8] Cheng X, Dai E, Wu J, Flores NM, Chu Y, et al. 2024. Atlas of metastatic gastric cancer links ferroptosis to disease progression and immunotherapy response. *Gastroenterology* 167:1345–1357

[9] Newman AM, Liu CL, Green MR, Gentles AJ, Feng W, et al. 2015. Robust enumeration of cell subsets from tissue expression profiles. *Nature Methods* 12:453–7

[10] Aran D, Hu Z, Butte AJ. 2017. xCell: digitally portraying the tissue cellular heterogeneity landscape. *Genome Biology* 18:220

[11] Becht E, Giraldo NA, Lacroix L, Buttard B, Elarouci N, et al. 2016. Estimating the population abundance of tissue-infiltrating immune and stromal cell populations using gene expression. *Genome Biology* 17:218

[12] Li B, Severson E, Pignon JC, Zhao H, Li T, et al. 2016. Comprehensive analyses of tumor immunity: implications for cancer immunotherapy. *Genome Biology* 17:174

[13] Finotello F, Mayer C, Plattner C, Laschober G, Rieder D, et al. 2019. Molecular and pharmacological modulators of the tumor immune contexture revealed by deconvolution of RNA-seq data. *Genome Medicine* 11:34

[14] Charoentong P, Finotello F, Angelova M, Mayer C, Efremova M, et al. 2017. Pan-cancer Immunogenomic Analyses Reveal Genotype-Immunophenotype Relationships and Predictors of Response to Checkpoint Blockade. *Cell Rep* 18:248–62

[15] Zeng D, Li M, Zhou R, Zhang J, Sun H, et al. 2019. Tumor microenvironment characterization in gastric cancer identifies prognostic and immunotherapeutically relevant gene signatures. *Cancer Immunology Research* 7:737–750

[16] Zeng D, Wu J, Luo H, Li Y, Xiao J, et al. 2021. Tumor microenvironment evaluation promotes precise checkpoint immunotherapy of advanced gastric cancer. *Journal for Immunotherapy of Cancer* 9:e002467

[17] Shi M, Zeng D, Luo H, Xiao J, Li Y, et al. 2024. Tumor microenvironment RNA test to predict immunotherapy outcomes in advanced gastric cancer: The TIMES001 trial. *Med* 5:1378–1392.e3

[18] Duan R, Li X, Zeng D, Chen X, Shen B, et al. 2020. Tumor microenvironment status predicts the efficacy of postoperative chemotherapy or

radiochemotherapy in resected gastric cancer. *Frontiers in Immunology* 11:609337

[19] Wang D, Wang N, Li X, Chen X, Shen B, et al. 2021. Tumor mutation burden as a biomarker in resected gastric cancer via its association with immune infiltration and hypoxia. *Gastric Cancer* 24:823–834

[20] Li Y, Li X, Yang Y, Qiao X, Tao Q, et al. 2023. Association of genes in hereditary metabolic diseases with diagnosis, prognosis, and treatment outcomes in gastric cancer. *Frontiers in Immunology* 14:1289700

[21] Tumeh PC, Harview CL, Yearley JH, Shintaku IP, Taylor EJM, et al. 2014. PD-1 blockade induces responses by inhibiting adaptive immune resistance. *Nature* 515:568–71

[22] Kzhyshkowska J, Shen J, Larionova I. 2024. Targeting of TAMs: can we be more clever than cancer cells? *Cellular & Molecular Immunology* 21:1376–1409

[23] Bai X, Guo YR, Zhao ZM, Li XY, Dai DQ, et al. 2025. Macrophage polarization in cancer and beyond: from inflammatory signaling pathways to potential therapeutic strategies. *Cancer Letters* 625:217772

[24] Kloosterman DJ, Akkari L. 2023. Macrophages at the interface of the co-evolving cancer ecosystem. *Cell* 186:1627–1651

[25] Jiang Y, Wang Y, Chen G, Sun F, Wu Q, et al. 2024. Nicotinamide metabolism face-off between macrophages and fibroblasts manipulates the microenvironment in gastric cancer. *Cell Metabolism* 36:1806–1822.e11

[26] Cantoni C, Falco M, Vitale M, Pietra G, Munari E, et al. 2024. Human NK cells and cancer. *Oncoimmunology* 13:2378520

[27] Netskar H, Pfefferle A, Goodridge JP, Sohlberg E, Dufva O, et al. 2024. Pan-cancer profiling of tumor-infiltrating natural killer cells through transcriptional reference mapping. *Nature Immunology* 25:1445–1459